

# ANALYSIS OF CISLUNAR TRANSFERS FROM A NEAR RECTILINEAR HALO ORBIT WITH HIGH POWER SOLAR ELECTRIC PROPULSION

Steven L. McCarty\*, Laura M. Burke†, Melissa L. McGuire‡

This paper captures analysis completed in an effort to design efficient cislunar transfers of a massive spacecraft from an L2 Southern NRHO to a Distant Retrograde Orbit, L1 Northern NRHO, and Flat L2 Halo Orbit using low thrust Solar Electric Propulsion (SEP). For each transfer type, a reference transfer is designed for an assumed 39 t spacecraft with 26.6 kW SEP system. For each reference transfer, analysis is completed to understand the sensitivity of the transfer to changes in initial mass and SEP power and to identify the optimal number of thrusters to use for a given combination of mass and power. The outlined approach of characterizing a trajectory by the acceleration and required thrusting time is shown to be useful in understanding a wide range of mass and power combinations. In addition to showing the inverse relationship between spacecraft acceleration and propellant mass, the analysis shows that regions in the trade space exist where additional SEP power is not useful for reducing the required propellant. Further, regions are identified where operating more thrusters at a lower specific impulse requires less propellant than operating fewer at a higher specific impulse.

## INTRODUCTION

As government and commercial interest in the exploration of the Moon and cislunar space has grown, Near Rectilinear Halo Orbits (NRHOs) have shown to be of particular interest as staging orbits for human exploration of the Moon,<sup>1-3</sup> and were previously the crew rendezvous orbit for the cancelled Asteroid Redirect Mission.<sup>4</sup> Once in such a staging orbit, low thrust solar electric propulsion (SEP) can enable efficient transfer to other multi-body orbits near the moon (in cislunar space).<sup>5</sup> There are many possible options for destination orbits in cislunar space depending on the objectives of the mission. The three particular cislunar destination orbits studied in this paper include a 70,000 km Distant Retrograde Orbit (DRO), an L1 Northern (L1N) NRHO, and a Flat Earth-Moon L2 Halo Orbit. These three orbits may be of interest for long-term stable storage, coverage of the lunar north pole, and ease of access, respectively. For each of these destinations, a one-way reference low thrust transfer has been designed to minimize propellant required for a transfer time of approximately 6 months.

The combination of a low thrust spacecraft in a dynamic multi-body environment makes designing efficient trajectories a challenge. Furthermore, a fluid spacecraft definition in early design

\*Mission Design Engineer, Mission Architecture and Analysis Branch, NASA Glenn Research Center, 21000 Brookpark Road, Cleveland, OH, 44135

†Aerospace Engineer, Mission Architecture and Analysis Branch, NASA Glenn Research Center, 21000 Brookpark Road, Cleveland, OH, 44135

‡Branch Chief, Mission Architecture and Analysis Branch, NASA Glenn Research Center, 21000 Brookpark Road, Cleveland, OH, 44135

phases can have a significant impact on the propellant required to complete a given low thrust transfer. Common design changes may include initial mass, power, and number of thrusters. To address this challenge, a straightforward method has been developed to characterize a given reference trajectory in order to understand the impact of these common design changes on propellant requirements. In addition to the impact on required propellant, the analysis of each of the reference trajectories provides insights that can inform design decisions regarding required SEP power and optimal number of thrusters for a given mass and power combination.

## GROUND RULES AND ASSUMPTIONS

As the needs and desires for the exploration of cislunar space change, so too do the ground rules and assumptions (GRA) that constrain the design of the reference trajectories. This section outlines the most recent GRA used in this work, including those for the spacecraft performance and the initial and destination cislunar orbits of interest.

### Spacecraft Assumptions

With an initial mass of 39,000 kg, the primary propulsion system of the spacecraft is assumed to be a high-power SEP system consisting of four 13.3 kW hall effect thrusters, with only two operating at a maximum of 26.6 kW at 1 au from the Sun. Available power is assumed to decrease as  $1/R^2$  when operating at distances greater than 1 au. In addition, perfect pointing is assumed for the arrays and no constraints are placed on the thrust direction. A duty cycle of 90% is used for all thrust arcs to provide margin for thrust outages and other non-thrusting activities, which is modeled by a proportionate decrease in thrust and mass flow rate. A summary of the spacecraft GRA is shown in Table 1.

The assumed performance for a single thruster as a function of input power is shown in Table 2. Available power is evenly distributed between all operating thrusters, with each operating at a minimum and maximum power of 7 kW and 13.3 kW, respectively.

**Table 1. Summary of the spacecraft ground rules and assumptions**

Parameter	Value	Note
Initial Mass	39,000 kg	Wet mass at start of transfer
Power	26.6 kW	Maximum at 1 au
Number of Thrusters	2+2	2 operating + 2 spare
Power Model	$1/R^2$	No increase in power for R less than 1 au
Duty Cycle	90%	For thrust outages and non-thrusting activities

**Table 2. SEP thruster performance as a function of input power**

Power (kW)	Thrust (mN)	$\dot{m}$ (mg/s)	$I_{sp}$ (s)
13.3	566.3	23.0	2,517
13.0	557.0	22.9	2,486
12.0	529.3	22.6	2,392
11.0	504.6	22.3	2,305
10.0	480.6	22.2	2,214
9.0	454.6	22.0	2,108
8.0	424.2	22.0	1,976
7.0	386.9	21.9	1,806

## Cislunar Orbit Assumptions

*Initial Orbit:* All trajectories presented depart from a 9:2 lunar synodic resonant southern L2 (L2S) NRHO, characterized by a perilune radius of approximately 3,233 km and a period of 6.6 days. This NRHO was selected based on favorable transfer characteristics as well as the ability to avoid lengthy eclipses by the Earth.<sup>2</sup> It exhibits nearly-stable behavior, and station-keeping algorithms enable long-term stays for either crewed or un-crewed assets.<sup>3</sup> This NRHO is considered a southern L2 halo orbit because its perilune is over the Moon's north pole and it spends most of its orbit above the Moon's south pole. This orbit is shown in blue in Figure 1.

For each departure, an optimally phased 9:2 NRHO is constructed by targeting a partial state in a Moon-centered Earth-Moon rotating frame and varying the free components to achieve zero x- and z-velocity at the y-axis crossing after half of a period. The targeted velocity is zero in the x- and z-direction and free in the y-direction, where x is along the Earth-Moon line and z is parallel to the angular momentum vector of the system. The targeted position is free in the x-direction, zero in the y-direction, and 3,230 km in the z-direction. This strategy provides a straightforward way to generate a representative 9:2 NRHO at any required epoch in the ephemeris model, though the resultant NRHO is not necessarily stable for more than one period in the ephemeris model.

*Destination 1:* The first destination orbit is a Distant Retrograde Orbit (DRO) with a radius of approximately 70,000 km from the Moon. DROs are known to be stable for periods of 100 years or more, making them an attractive location for potential spacecraft disposal or long-term storage in cislunar space. This type of orbit was considered as a final storage orbit for the asteroid that was to be returned by the Asteroid Redirect Robotic Mission.<sup>4</sup> This orbit is shown in green in Figure 1.

For arrival to the DRO, an optimally phased 70,000 km DRO is constructed by targeting a partial state in a Moon-centered Earth-Moon rotating frame and varying the free components to achieve zero x-velocity at the y-axis crossing with an appropriate period. The targeted velocity is zero in the x- and z-direction and free in the y-direction, where x is along the Earth-Moon line and z is parallel to the angular momentum vector of the system. The targeted position is -70,000 km in the x-direction and zero in the y- and z-direction. This strategy provides a straight-forward way to generate a representative DRO at any required epoch in the ephemeris model, though long term stability is not guaranteed.

*Destination 2:* The second destination orbit is a northern L1 (L1N) NRHO, characterized by a perilune radius of 3,750 km and a period of 7.1 days. This NRHO provides similar characteristics as the initial L2S, though not necessarily the eclipse benefit without a targeted lunar synodic resonance. Being a northern NRHO, this orbit provides extended coverage of the northern hemisphere of the Moon. An optimally phased L1N NRHO is constructed used a method similar to that used for the initial NRHO. This orbit is shown in red in Figure 1.

*Destination 3:* The final destination orbit is a Flat L2 Halo Orbit, characterized by a z-amplitude of approximately 3,500 km and a period of approximately 15 days. The Flat L2 Halo Orbit was chosen for its attractiveness as a staging orbit to other destinations because it possesses stable and unstable manifolds that can provide low cost transfers to Earth, other orbits in cislunar space and beyond. An optimally phased Flat L2 Halo Orbit is constructed used a method similar to that used for the initial NRHO. This orbit is shown in black in Figure 1.

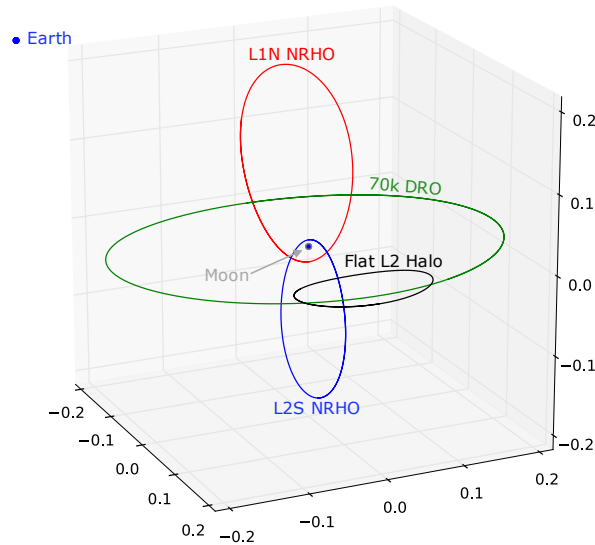


**Figure 1. Overview of the cislunar orbits of interest in the Earth-Moon rotating frame. The initial L2S NRHO is shown in blue and the destination DRO, L1N NRHO and Flat L2 Halo Orbit are shown in green, red and black, respectively.**

## REFERENCE CISLUNAR TRANSFERS

A reference transfer has been designed from the initial NRHO to each of the cislunar destination orbits. For each, the transfer time of flight (TOF) was chosen to be 6 months or less as a compromise between fast, expensive transfers, and very long duration, more efficient options. The optimization objective is maximum final mass, which is equivalent to minimum propellant mass in these cases. All transfers use the DE430 ephemeris model and include point mass gravity for the Earth, Moon and Sun. The transfers were designed using Copernicus,<sup>6</sup> a high-fidelity trajectory optimization tool, with a parallel monotonic basin hopping wrapper.<sup>7</sup>

### L2S NRHO to DRO

The reference transfer from the initial NRHO to the destination DRO is shown in Figure 2. This transfer consists of 5 thrust arcs, with the first two used to depart the NRHO and lunar vicinity. The primary challenge for the transfer from the NRHO to DRO is the plane change required, as the NRHO and DRO are nearly perpendicular to one another. A single revolution around the earth, in the Earth-Moon rotating frame, is followed by a targeted lunar gravity assist on the return approach to the Moon in order to complete this plane change before entering into the DRO. The final 13.7 day thrust arc is used to capture into the destination DRO. A relatively long thrust arc is generally required to capture into the DRO due to its stable characteristics. In total, this transfer requires 155.7 days and 134.9 kg of propellant (85 m/s SEP  $\Delta V$ ). A summary of the event timeline throughout the transfer is shown in Table 3.

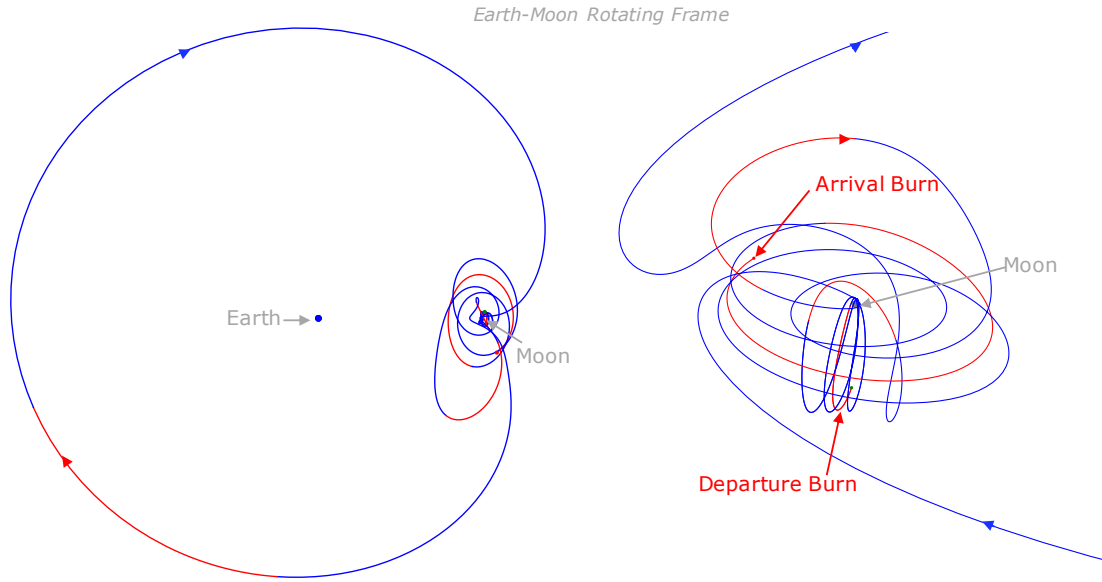


**Figure 2. Overview (left) and close up view (right) of the L2S NRHO to DRO transfer displayed in the Earth-Moon rotating frame. Coast and thrust arcs are colored in blue and red, respectively.**

**Table 3. Event summary for the reference L2S NRHO to DRO transfer**

Date	Event	MET (d)	$\Delta t$ (d)	Mass (kg)	Prop. (kg)	$R_{\text{Moon}}$ (km)
2025-01-07	Departure	0.0	-	39,000.0	-	50,275
2025-01-07	Thrust 1	0.0	4.9	39,000.0	17.5	50,275
2025-01-12	Coast 1	4.9	20.3	38,982.5	-	8,838
2025-02-01	Thrust 2	25.2	2.2	38,982.3	7.8	39,399
2025-02-04	Coast 2	27.5	29.2	38,974.5	-	41,913
2025-03-05	Thrust 3	56.7	8.0	38,974.4	28.6	786,254
2025-03-13	Coast 3	64.7	28.3	38,945.8	-	1,076,813
2025-04-10	Thrust 4	92.9	9.0	38,945.7	31.9	71,838
2025-04-19	Coast 4	101.9	40.1	38,913.7	-	243,999
2025-05-29	Thrust 5	142.0	13.7	38,913.7	48.7	115,672
2025-06-12	Arrival	155.7	-	38,865.1	-	88,791

## L2S NRHO to L1N NRHO

The reference transfer from the initial L2S NRHO to the destination L1N NRHO is shown in Figure 3. This transfer consists of 4 thrust arcs, with the first two used to depart the NRHO and lunar vicinity. A single revolution around the earth, in the Earth-Moon rotating frame, is followed by a second revolution interior to the Moon's orbit before the final approach to the Moon. The final 2.6 day thrust arc is used to capture into the destination L1N NRHO. In total, this transfer requires 159.7 days and 67.4 kg of propellant (43 m/s SEP  $\Delta V$ ). A summary of the event timeline throughout the transfer is shown in Table 4.

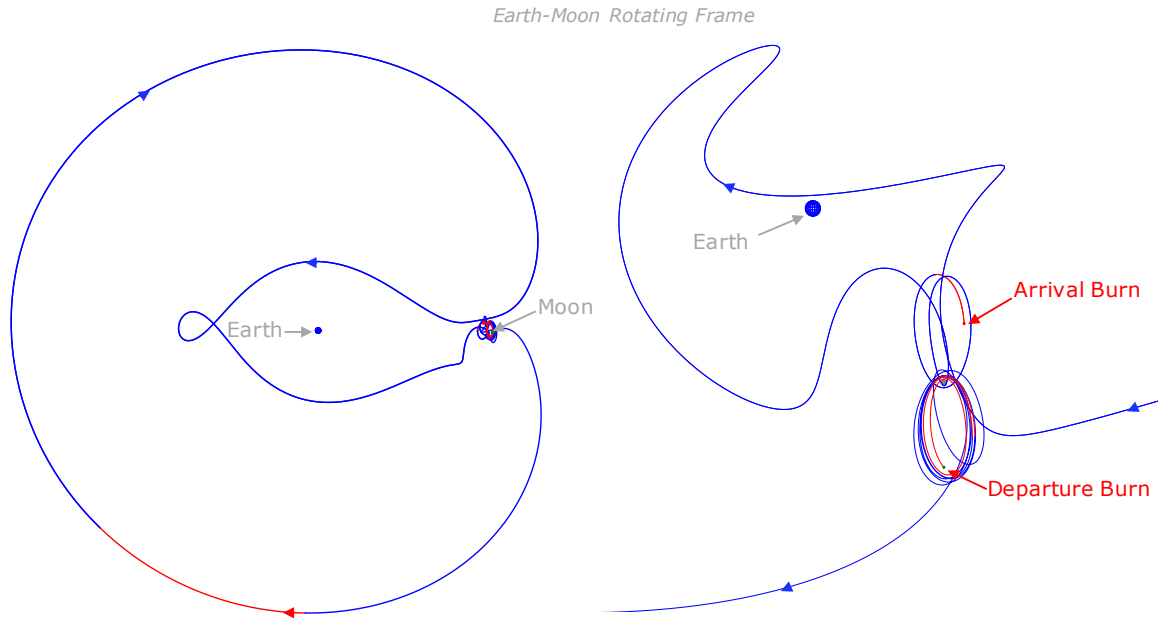


**Figure 3. Overview (left) and close up view (right) of the L2S NRHO to L1N NRHO transfer displayed in the Earth-Moon rotating frame. Coast and thrust arcs are colored in blue and red, respectively.**

**Table 4. Event summary for the reference L2S NRHO to L1N NRHO transfer**

Date	Event	MET (d)	$\Delta t$ (d)	Mass (kg)	Prop. (kg)	$R_{\text{Moon}}$ (km)
2024-12-24	Departure	0.0	-	39,000.0	-	63,998.8
2024-12-24	Thrust 1	0.0	9.8	39,000.0	35.1	63,998.8
2025-01-02	Coast 1	9.8	5.5	38,964.9	-	47,906.5
2025-01-08	Thrust 2	15.4	1.3	38,964.9	4.8	10,380.3
2025-01-09	Coast 2	16.7	53.0	38,960.1	-	48,724.1
2025-03-03	Thrust 3	69.6	5.0	38,960.1	18.2	771,904.5
2025-03-08	Coast 3	74.7	82.5	38,941.9	-	987,405.0
2025-05-30	Thrust 4	157.1	2.6	38,941.9	9.3	80,188.4
2025-06-01	Arrival	159.7	-	38,932.6	-	46,057.6

## NRHO to Flat L2 Halo Orbit

The reference transfer from the initial L2S NRHO to the destination Flat L2 Halo Orbit is shown in Figure 4. This transfer consists of 3 thrust arcs, with the first used to depart the NRHO and lunar vicinity. Three exterior revolutions around the earth, in the Earth-Moon rotating frame, are completed before the final approach to the Moon. The final 0.1 day thrust arc is used to capture into the destination Flat L2 Halo Orbit. The relatively small arrival thrust arc is possible due to the stability characteristics of the target orbit. In total, this transfer requires 169.5 days and 117.3 kg of propellant (74 m/s SEP  $\Delta V$ ). A summary of the event timeline throughout the transfer is shown in Table 5.

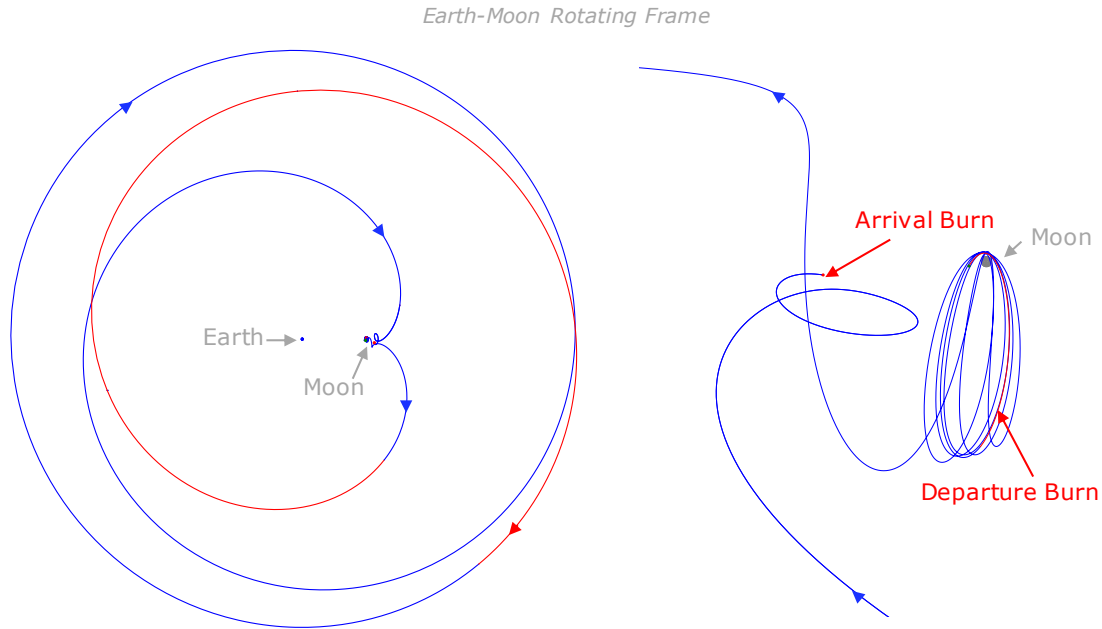


**Figure 4. Overview (left) and close up view (right) of the L2S NRHO to Flat L2 Halo Orbit transfer displayed in the Earth-Moon rotating frame. Coast and thrust arcs are colored in blue and red, respectively.**

**Table 5. Event summary for the reference L2S NRHO to Flat L2 Halo Orbit transfer**

Date	Event	MET (d)	$\Delta t$ (d)	Mass (kg)	Prop. (kg)	$R_{\text{Moon}}$ (km)
2024-12-25	Departure	0.0	-	39,000.0	-	8,774
2024-12-25	Thrust 1	0.0	2.2	39,000.0	7.9	8,774
2024-12-28	Coast 1	2.2	58.1	38,992.1	-	63,949
2025-02-24	Thrust 2	60.3	30.6	38,992.1	109.2	742,805
2025-03-26	Coast 2	90.9	78.5	38,882.8	-	1,529,756
2025-06-13	Thrust 3	169.4	0.1	38,882.8	0.2	58,578
2025-06-13	Arrival	169.5	-	38,882.7	-	58,273

## POWER AND MASS SENSITIVITY

Each reference trajectory outlined above was designed with a specific initial spacecraft mass, SEP power, and number of thrusters (39,000 kg, 26.6 kW, and 2, respectively). As such, each solution is specific to that spacecraft configuration and cannot readily inform how a somewhat different configuration may perform. For example, a less massive spacecraft would be capable of a higher initial acceleration, but it is not clear how that would translate to propellant savings. Further, additional SEP power could increase the initial spacecraft acceleration, but there will exist regions in the trade space where additional power will require additional thrusters, all of which would then be run at a lower specific impulse ( $I_{sp}$ ). It is not immediately obvious whether this results in improved performance for a given transfer. Lastly, if a combination of initial mass, power, and thrusters is chosen that significantly decreases the initial spacecraft acceleration, there exists a point at which the transfer type is no longer feasible without increasing the TOF.

The goal of this analysis is to address some of these uncertainties by understanding how changes in initial spacecraft mass, power, and number of thrusters impact the propellant required for the transfer. To that end, a method was pursued that allows a relatively small dataset generated with a specific spacecraft configuration to be decoupled from that configuration. With a few reasonable approximations, to be outlined in this section, the generated dataset can be safely interpolated and applied to additional configurations falling within its bounds. The following process is applied separately to each reference trajectory.

For each reference transfer, a continuation method is used to generate a similar trajectory for a range of initial spacecraft accelerations by increasing the spacecraft initial mass in 1,000 kg steps. This process is continued until feasible solutions are no longer possible for the given transfer type, corresponding to the minimum spacecraft acceleration capable of completing the transfer. Similarly, the initial mass from the reference transfer is decreased in 1,000 kg steps until reaching what is considered a reasonable maximum expected initial spacecraft acceleration. It should be noted, however, that any acceleration above the minimum threshold would result in a feasible solution. Care is taken to ensure the geometry of the transfer, including the total TOF, remains similar for all solutions.

Once this dataset is assembled, a polynomial curve fit can be generated for the total thruster-on time as a function of initial spacecraft acceleration (calculated as the thrust divided by the initial spacecraft mass). The dataset and associated polynomial fits are shown in Figure 5. Displaying the data for all transfers on one plot shows the relative sensitivity of each. As acceleration decreases from the reference, required thrusting time can quickly grow for the DRO transfer. The Flat L2 Halo Orbit displays similar behavior to the DRO, but can support lower accelerations before a sharp increase in thrusting time occurs. The LIN NRHO transfer curve remains relatively flat, indicating that reducing acceleration does not drastically increase the required thrusting time. With these curves, the required thruster-on time can then be calculated for any initial acceleration, which is itself a function of the initial mass, power, and number of thrusters. The chosen power and number of thrusters determines the thrust magnitude, which is then divided by the chosen spacecraft mass to determine the initial acceleration. The propellant mass is then calculated by multiplying the total thruster-on time by the mass flow rate of the SEP system as determined by the chosen power, number of thrusters, and thruster performance curve.

The choice of number of thrusters to operate, 2 or 3 in this case, will determine the thrust and  $I_{sp}$  of the SEP system. To better illustrate the impact of this choice, Figure 6 shows plots of thrust



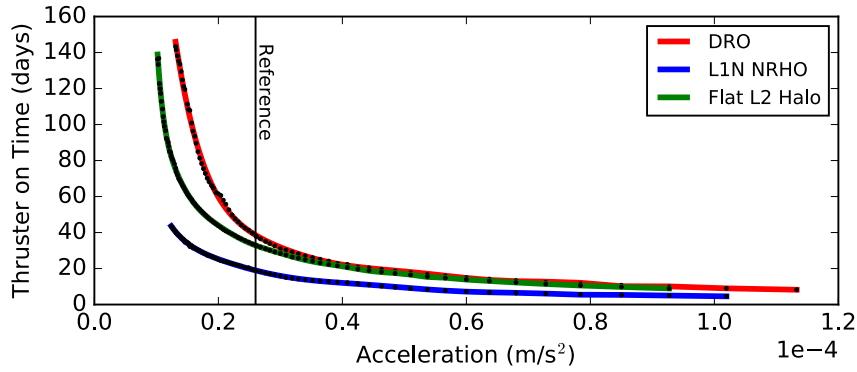


**Figure 5. Plot of required thruster-on time as a function of initial spacecraft acceleration for each transfer type. Discrete data points are shown in black and a polynomial curve fits are shown in red, blue, and green for the DRO, L1N NRHO, and Flat L2 Halo Orbit, respectively. A vertical black line indicates the acceleration of the reference trajectories**

and  $I_{sp}$  as a function of input power for 2 or 3 thrusters, assuming all available power is evenly distributed between thrusters. These plots demonstrate the tradeoff between switching between 2 and 3 thrusters when enough power is available to do so, above 21 kW. For example, at the maximum 2-thruster input power of 26.6 kW, switching to 3 thrusters would provide approximately 20% more thrust, but the resultant  $I_{sp}$  would decrease by 20%. The optimal number of thrusters to choose for a given transfer will therefore depend upon the sensitivity of the transfer to changes in acceleration. If a 20% increase in thrust, equivalent to a 20% increase in acceleration for a fixed mass, can reduce the required thrusting time enough to make up for the decrease in  $I_{sp}$ , then 3-thruster operation will require less propellant. Otherwise, 2-thruster operation will be preferred. The choice depends upon the operating point and behavior of the transfer in Figure 5.

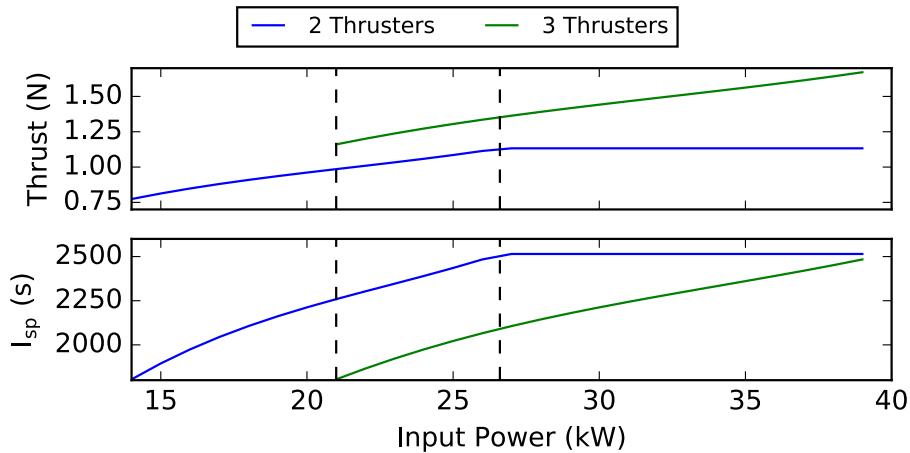


**Figure 6. Plots of thrust (top) and  $I_{sp}$  (bottom) as a function of input power for 2 or 3 thrusters, plotted in blue and green, respectively. The 3-thruster maximum power (21 kW) and 2-thruster maximum power (26.6 kW) are marked with dashed vertical lines.**

This approach introduces two approximations. First, the polynomial curve fit is an approximation of the true behavior of the dataset, but a fine enough point resolution with a well fit curve can minimize the error introduced. In addition, ensuring that chosen configurations generate accelerations between the bounds of the dataset means that the values are interpolated between actual trajectories rather than extrapolated to unmodeled regions. Second, this approach ignores the change in acceleration throughout the transfer (via decremented propellant mass). For this analysis, the error introduced by ignoring the change in acceleration is acceptable because the total mass of the spacecraft is much greater than the mass of the propellant used. In the edge cases, it is expected that the spacecraft acceleration changes by less than 1%, which is itself a conservative error because spacecraft acceleration would increase as propellant mass is expelled.

## **L2S NRHO to DRO**

Using the approach outlined above, the contour plot in Figure 7 is generated. This plot shows contours of propellant mass required to complete the transfer for combinations of SEP power from 14 to 39.9 kW (2-thruster minimum power and 3-thruster maximum power) and initial masses from 39 to 100 t. For each point, the propellant required was calculated for 2 and 3 thrusters. Vertical black lines indicate the minimum power for 3 thrusters (21 kW) and the maximum power for 2 thrusters (26.6 kW). The grey region in the upper left corner corresponds to combinations of mass and power that lead to an acceleration that is too low to complete the transfer with either 2 or 3 thrusters. Regions where 2 thrusters require less propellant than 3 thrusters are shaded in blue ("2 Thrusters More Efficient"). Regions where 3 thrusters require less propellant than 2 thrusters are shaded in green ("3 Thrusters More Efficient"), and regions where 3 thrusters are required, because 2 thrusters do not provide enough thrust, are shaded in purple ("3 Thrusters Required").

It should be noted that unexpected behavior can occur directly along the transition between blue and green regions because the difference between the propellant required with 2 and 3 thrusters approaches zero. Also, near the transition, the propellant difference between 2 and 3 thrusters is considered to fall within the noise of the data points used to generate the acceleration curves. In an effort to more cleanly define this transition, the green regions actually identify regions where switching to 3 thrusters results in a savings of at least 5 kg or 3% compared to 2 thrusters. To be safe, if a design point is chosen close to this transition, additional analysis should be performed to determine the preferred number of thrusters.

With that said, a number of interesting conclusions can be drawn from Figure 7. First, for the reference power level of 26.6 kW, feasible transfers are available for initial masses up to approximately 90 t if using 3 thrusters. If limited to 2 thrusters, the maximum initial mass is approximately 75 t. In either case, the required propellant mass increases dramatically, from the reference of 134.9 kg to 500+ kg. Also of interest is the blue region that exists for power levels greater than 26.6 kW, which corresponds to a region where additional power is not actually of benefit because it would require more propellant to operate three thrusters at a lower  $I_{sp}$ , despite the increase in thrust. The additional power is not used since the two thrusters are already operating at maximum power. As power continues to increase, the green region is reached where 3-thruster operation is more efficient because enough power is available to operate all thrusters at a high enough  $I_{sp}$ , as determined by the thruster performance curves. The plot also shows that transfers are feasible with SEP power of only 14 kW (2-thruster minimum) as long as initial mass is below approximately 53 t. Finally, the contours can be used to determine the feasible combinations of mass and power for a constrained propellant mass. For example, if no more than 200 kg of propellant can be reserved for the transfer,

the spacecraft configuration must be in the region below the 200 kg contours. As will be seen in comparison to the other reference transfers, the propellant required to complete this L2S NRHO to DRO transfer is relatively sensitive to the initial spacecraft acceleration in the region of interest. This can also be seen clearly in in Figure 5, where small changes in acceleration can correspond to large changes in thruster-on time.

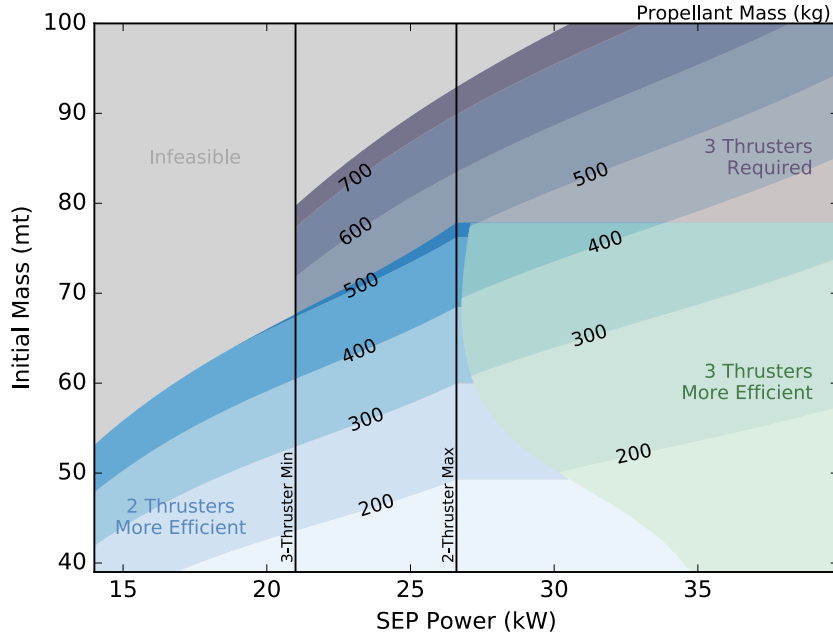


**Figure 7. Contour plot of propellant required to complete the L2S NRHO to DRO transfer for a chosen combination of SEP power and initial mass. Regions where 2-thruster operation is most efficient are shown in blue, regions where 3-thruster operation is more efficient are overlaid in green, and regions where 3-thruster operation is required are shown in purple.**

## L2S NRHO to L1N NRHO

Using the approach outlined above, the contour plot in Figure 8 can be generated for the L1N NRHO transfer (see the previous L2S NRHO to DRO section for a detailed plot explanation). A number of interesting conclusions can be drawn from this plot. First, for the reference power level of 26.6 kW, feasible transfers are available for initial masses up to approximately 97 t if using 3 thrusters. If limited to 2 thrusters, the maximum initial mass is approximately 80 t. In either case, the required propellant mass increases relatively modestly from the reference of 80 kg to 175+ kg. Also of interest is the blue region that exists for power levels greater than 26.6 kW, which corresponds to a region where additional power is not actually of benefit because it would be less efficient to operate three thrusters at a lower  $I_{sp}$  despite the increase in thrust. The additional power is not used since the two thrusters are already operating at maximum power. As power and mass increase, a small green region exists where the 3-thruster operation is more efficient because enough power is available to operate all thrusters at a high enough  $I_{sp}$ , as determined by the thruster performance curves. The plot also shows that transfers are feasible with SEP power of only 14 kW (2-thruster minimum) as long as initial mass is below approximately 56 t. Finally, the contours can

be used to determine the feasible combinations of mass and power for a constrained propellant mass. For example, if no more than 100 kg of propellant can be reserved for the transfer, the spacecraft configuration must be in the region below the 100 kg contours. Compared to the DRO transfer, the propellant required to complete this L2S NRHO to L1N NRHO transfer is less sensitive to the initial spacecraft acceleration. This can also be seen clearly in in Figure 5, where small changes in acceleration can correspond to relatively modest changes in thruster-on time.

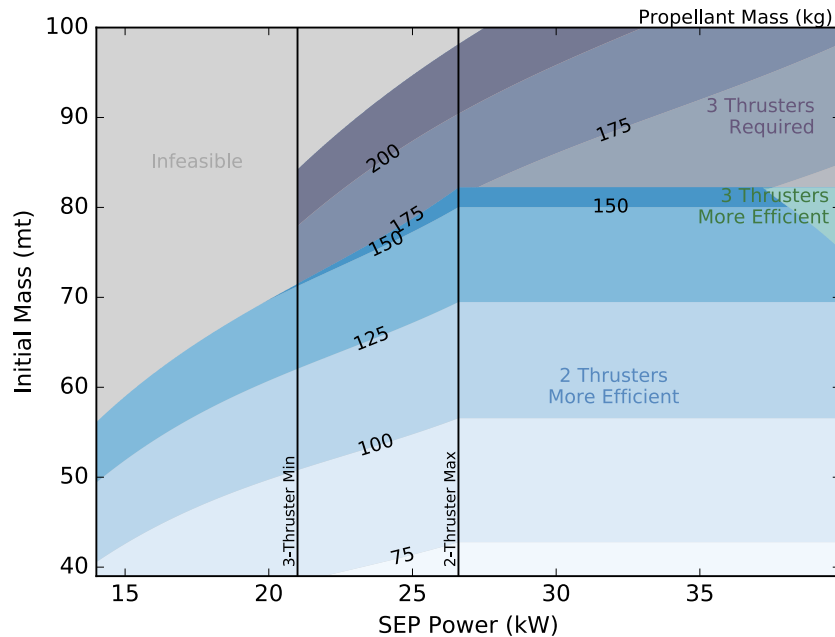


**Figure 8. Contour plot of propellant required to complete the L2S NRHO to L1N NRHO transfer for a chosen combination of SEP power and initial mass. Regions where 2-thruster operation is more efficient are shown in blue, regions where 3-thruster operation is more efficient are overlaid in green, and regions where 3-thruster operation is required are shown in purple.**

### L2S NRHO to Flat L2 Halo Orbit

Using the approach outlined above, the contour plot in Figure 9 is generated (see the previous L2S NRHO to DRO section for a detailed plot explanation). A number of interesting conclusions can be drawn from this plot. First, it can be seen that, for the reference power level of 26.6 kW, the initial mass can be greater than 100 t with either 2 or 3 thrusters, though a region exists where 3 thrusters is more efficient even though not required. Also of interest is the blue region that exists for power levels greater than 26.6 kW, which corresponds to a region where additional power is not actually of benefit because it would be less efficient to operate three thrusters at a lower  $I_{sp}$  despite the increase in thrust. The additional power is not used since the two thrusters are already operating at maximum power. As power and mass increase, a green region exists where the 3-thruster operation is more efficient because enough power is available to operate all thrusters at a high enough  $I_{sp}$ , as determined by the thruster performance curves. The plot also shows that transfers are feasible with SEP power of only 14 kW (2-thruster minimum) as long as initial mass is below approximately 68 t. Finally, the contours can be used to determine the feasible combinations

of mass and power for a constrained propellant mass. For example, if no more than 150 kg of propellant can be reserved for the transfer, the spacecraft configuration must be in the region below the 150 kg contours. Compared to the L1N NRHO transfer, the propellant required to complete this L2S NRHO to Flat L2 Halo Orbit transfer is more sensitive to the initial spacecraft acceleration. This can also be seen clearly in in Figure 5, where small changes in acceleration can correspond to more dramatic changes in thruster-on time.

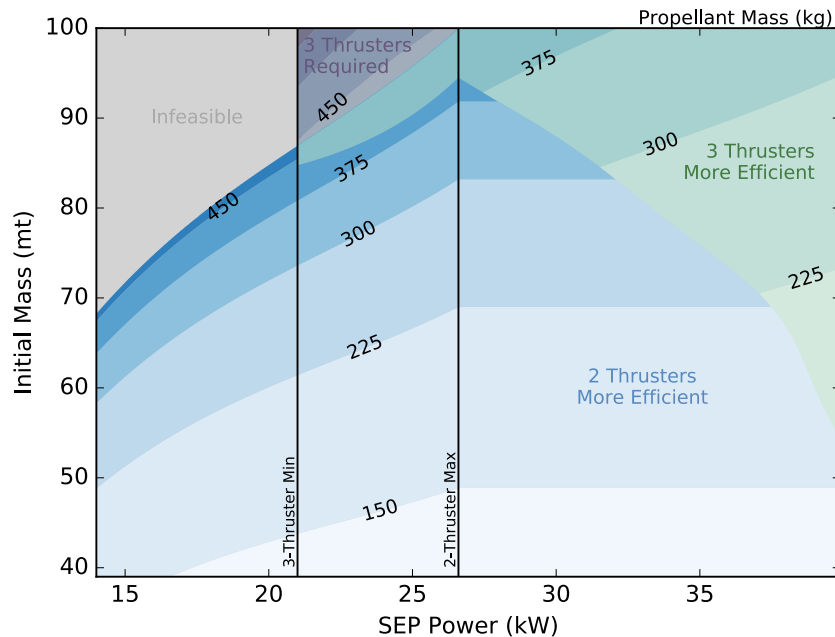


**Figure 9. Contour plot of propellant required to complete the NRHO to Flat L2 Halo Orbit transfer for a chosen combination of SEP power and initial mass. Regions where 2-thrust operation is most efficient are shown in blue, regions where 3-thruster operation is more efficient are overlaid in green, and regions where 3-thruster operation is required are shown in purple.**

## CONCLUSION

The results presented above demonstrate that SEP can be used to efficiently transfer a large spacecraft between cislunar orbits. Reference trajectories have been designed to transfer from an initial L2S NRHO to three different cislunar orbit destination of interest in approximately 6-months total TOF. The use of an efficient SEP system enables the transfer of a 39,000 kg spacecraft with just 67 - 135 kg of propellant (43 - 85 m/s  $\Delta V$ ).

The L2S NRHO to DRO transfer was found to be the most sensitive to changes in spacecraft acceleration, either through decreased power or increased mass. The L2S NRHO to Flat L2 Halo Orbit showed similar behavior to the DRO transfer, but can support lower accelerations before a sharp increase in thrusting time is observed. Lastly, the L2S NRHO to L1N NRHO was shown to be the least sensitive transfer, with a relatively flat relationship between acceleration and thrusting in the range of spacecraft accelerations considered.

The method of characterizing a transfer type by the required acceleration enables insight into

the system and understanding of the sensitivities without needing to create an optimal trajectory for every single case. In addition to determining the propellant required for a chosen spacecraft configuration, the analysis helps to identify the preferred number of active thrusters for the given SEP power and initial mass. It was found that additional power cannot always be utilized because doing so would require operating more thrusters at a lower efficiency, which negates the savings from a decrease in thruster-on time enabled by the increase in thrust. Also, regions are identified where 3 thrusters are required to complete the transfer when 2 thrusters do not provide enough thrust. Lastly, this method enables the identification of a maximum possible initial mass for a given transfer type, though greater masses are likely possible with increased TOF.

## REFERENCES

- [1] D. J. Grebow, M. T. Ozimek, K. C. Howell, and D. C. Folta, "Multi-Body Orbit Architectures for Lunar South Pole Coverage," *16th AAS/AIAA Space Flight Mechanics Conference*, January 2006.
- [2] R. Whitley and R. Martinez, "Options for Staging Orbits in Cis-Lunar Space," *37th IEEE Annual Aerospace Conference*, March 2016.
- [3] J. Williams, D. E. Lee, R. J. Whitley, K. A. Bokelmann, D. C. Davis, and C. F. Berry, "Targeting Cislunar Near Rectilinear Halo Orbits for Human Space Exploration," *27th AAS/AIAA Space Flight Mechanics Meeting*, February 2017.
- [4] M. L. McGuire, N. J. Strange, L. M. Burke, S. L. McCarty, G. B. Lantoine, M. Qu, H. Shen, D. A. Smith, and M. A. Vavrina, "Overview of the Mission Design Reference Trajectory for NASA's Asteroid Redirect Robotic Mission," *AAS/AIAA Astrodynamics Specialist Conference*, August 2017.
- [5] M. L. McGuire, L. M. Burke, S. L. McCarty, K. J. Hack, R. J. Whitley, D. C. Davis, and C. Ocampo, "Low Thrust Cis-Lunar Transfers Using a 40 kW-Class Solar Electric Propulsion Spacecraft," *AAS/AIAA Astrodynamics Specialist Conference*, August 2017.
- [6] C. Ocampo and J. Senent, "The Design and Development of COPERNICUS: A Comprehensive Trajectory Design and Optimization System," *57th International Astronautical Congress*, October 2006.
- [7] S. L. McCarty and M. L. McGuire, "Parallel Monotonic Basin Hopping for Low Thrust Trajectory Optimization," *28th AIAA/AAS Space Flight Mechanics Meeting*, January 2018.